Data Article

Dataset on the DFT-QSAR, and docking approaches for anticancer activities of 1, 2, 3-triazole-pyrimidine derivatives against human esophageal carcinoma (EC-109)

Rhoda Oyeladun Adegoke [a], Abel Kolawole Oyebamiji [a,b], Banjo Semire [a,*]

[a] Department of Pure and Applied Chemistry, Faculty of Pure and Applied Sciences, Ladoke Akintola University of Technology, Ogbomoso, Oyo State, Nigeria
[b] Department of Basic Sciences, Adeleke University, P.M.B. 250, Ede, Osun State, Nigeria

ABSTRACT

The investigation of the novel hybrid, 1, 2, 3-triazole moiety combined with pyrimidine derivatives against human esophageal carcinoma is an unexplored field of theoretical/computational chemistry. Also, the development of new drugs still remains a major challenge, cost-intensive and time-consuming, thus making the computational approach now a hot topic due to its ability to hasten up and aid the process of drug designs. Here, the use of the quantum chemical method via density functional theory (DFT) was employed in calculating molecular descriptors for developing the quantitative structure-activity relation (QSAR) model which predicts bioactivity of the selected 1, 2, 3-triazole-pyrimidine derivatives. Quantum chemical method implemented in Spartan 14, was used in calculating the molecular descriptors. The obtained results were imputed into Gretl and SPSS (software package for social sciences) to generate a novel QSAR model equation for human esophageal carcinoma (EC-109) through multiple linear regression. The relationship between the experimental and predicted inhibition efficiency (IC_{50}) of 1,2,3-triazole-pyrimidine with EC-109 was calculated which gives good correlation results. QSAR was validated using
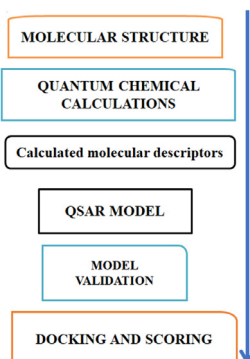
* Corresponding author.
   E-mail address: bsemire@lautech.edu.ng (B. Semire).

CV.R^2 and R_a^2. Fitting value (R^2) of 0.999 with an adjusted fitting value (R_a^2) of 0.995 was obtained and the result of validating QSAR performance gave CV.R^2 and R_a^2 value that is greater than 0.6, signifying its appropriateness and dependability. Molecular docking through simulation using Discovery Studio 4.1, Autodock Tool 1.5.6 and AutodockVina 1.1.2 was also carried out to calculate the free energy of ligand-receptor interactions as well as ligand conformation in the receptor-binding site. The results obtained revealed the presence of hydrogen bond interaction of the ligands with the amino acids residue in the binding sites of the receptor. Conformation of the ligands was essential property for binding ligand with the receptor. Critical examination and the correlations between the IC$_{50}$ and binding energy showed the activeness of ligand conformation in the gouge of the receptor with binding energy greater than the 5-fluorouracil (5- Fu) that was used as the standard compound.

Specification table

Subject	Physical Chemistry, Computational Chemistry
Specific subject area	Drug discovery
Type of data	Table
	Figure
	Model equation
How data were acquired	Quantum chemical calculations, QSAR modeling, docking, binding energy, and molecular visualization
Data format	Raw
	Analyzed (Observed (i.e. experimental) and Predicted)
Parameters for data collection	Spartan 14, DFT, Gretl, Discovery studio 4.1, Autodock tool 1.5.6 and Autodock vina 1.1.2, Pymol 1.7.4.4
Description of data collection	
Data source location	Ladoke Akintola University of Technology, Ogbomoso
Data accessibility	Data can be accessed with the article (Tables 1–4 and Figs. 1–5) and in the supporting information

Value of the data

- Datasets in this work will benefit researchers in predicting molecular properties from the molecular structures without the need to perform experiments that are costly and time-consuming.
- Datasets in this article will help in applying computational power to be combined chemically and biologically in order to streamline from optimization, development, design, and drug discovery.
- The additional value of the data results of QSAR and also the interactions between functional groups in the molecules of greatest activity can be understood.
- Using *in silico* screening tools, predictions of drug responses can significantly contribute to preclinical researches which are purely computational. The tools that can help biologists to prioritize and strategize their researches for candidate compounds, which are of great benefit for resourceful experimental planning and costs reduction.
- The improvement of accurate and computational efficiency are two important reasons for the continuous interest in the development of new, efficient, reliable, numerical stability, and modularly designed methods in the quantum theory of the atomic nuclei and the electrons.

1. Data description

Table 1 presents the schematic structure and names of investigated 1, 2, 3-triazole-pyrimidine hybrids, showing the twenty (20) minimized and optimized compounds. These were further employed in performing quantum calculations for the molecular descriptors, QSAR modeling, and docking simulations. The compound consists of 20 derivatives (Table 1) taken from Ma et al. [1].

Tables SI 1 and 2 (in the supporting information) present the datasets of the selected molecular parameters obtained by B3LYP/6–31G** using DFT [2]. The molecular descriptors extracted were based on the electronic properties of the investigated compounds. The descriptors include HOMO, LUMO, HOMO-LUMO, chemical hardness, band gaps, solvation energy, chemical potential, area volumes, diploe moments, softness, global nucleophilicity, ovality, log P, polar surface areas, polarizability, hydrogen bond donors, hydrogen bond acceptors, an average of Mulliken charges on all heteroatoms and number of organic atom.

Table 2 presents the 20 compounds with their corresponding fitting datasets for the predicted IC_{50} and the experimental IC_{50} for EC-109, showing that the predicted IC_{50} fitted well into the observed IC_{50} and this explicitly revealed that the developed QSAR model replicated the experimental bioactivity of the compound under consideration.

Fig. 1 presents the correlation between predicted and observed IC_{50} for EC-109, which shows that the QSAR model developed linked the activities of the compounds to their biological activities, and that the calculated IC_{50} fitted well into the observed IC_{50}. Moreover, statistical analyses are carried out, the correlation coefficient (R^2), gave 0.999 indicating a very good fit; as well as the effectiveness of the developed QSAR model to predict the anti-Esophageal cancer activity of triazole-pyrimidine compounds as shown in Eq. (1) generated for EC-109 inserted in Table 3. The calculated cross-validation ($CV.R^2$) was 0.999 which shows its reliability and acceptability because the value obtained is greater than 0.5 [3,4]. Also, the predicting power of the QSAR model developed was believed to be enhanced, since adjusted correlation coefficient (R^2_a) was calculated to be 0.995 which is greater than 0.6 [2] as presented in Table 3.

Fig. 2 shows the treatment of raw receptor and removal of water molecules and other residues apart from the target compounds using the Discovery studio. Fig. 3 presents the transparent views of docked complexes showing ligand-receptor interactions in the binding pocket for the best selected active compounds (**L1, L4, L6, L11, L15, L16, L17, L18, L19,** and **L20**) against EC-109 (receptor) using Pymol which was based on the lowest IC_{50} in the range of $\leq 10\,\mu M$

Table 1
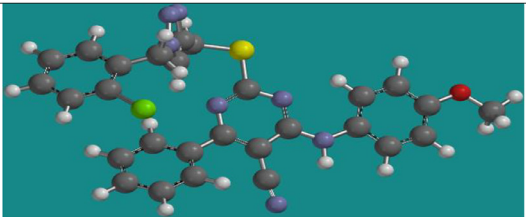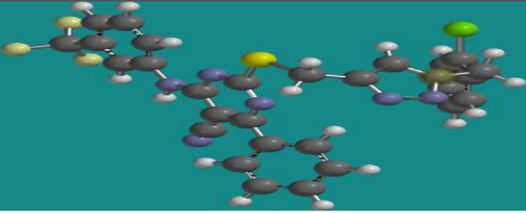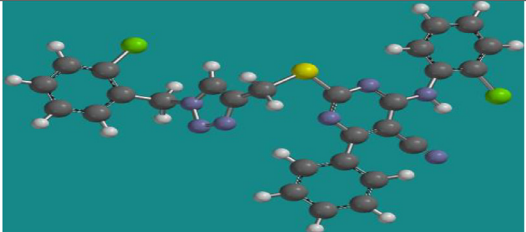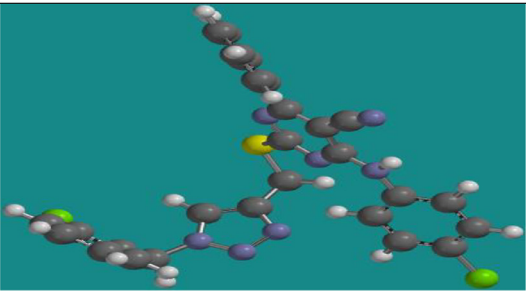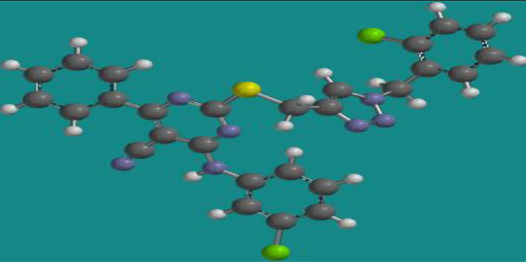Schematic structure and names of 1, 2, 3-triazole-pyrimidine hybrids.
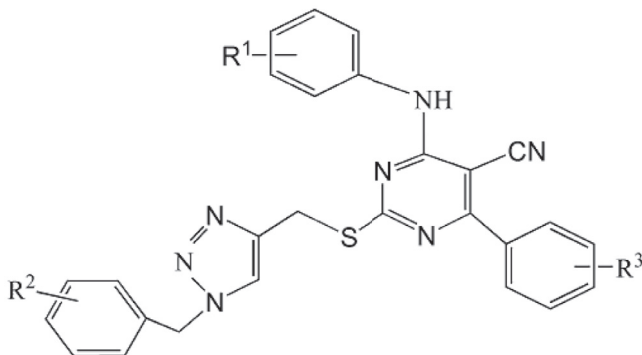
1, 2, 3-triazole-pyrimidine hybrids
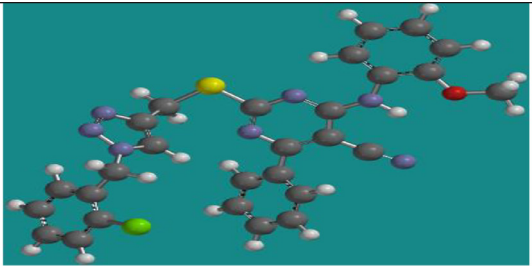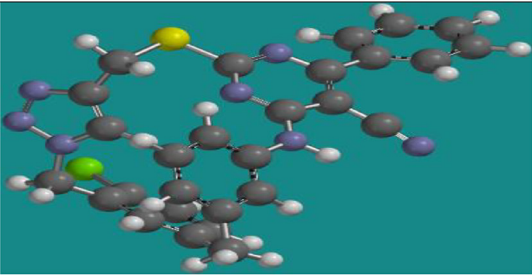
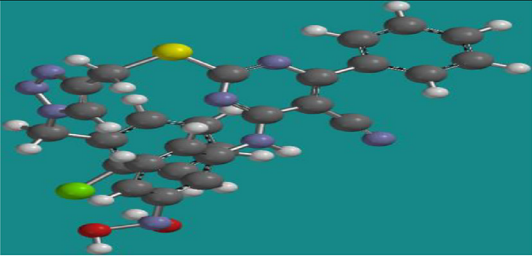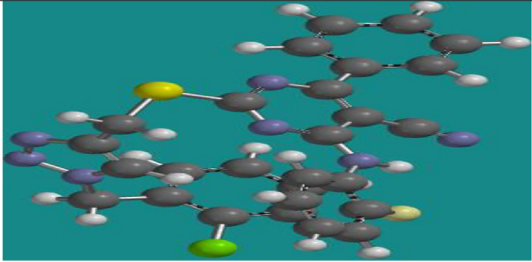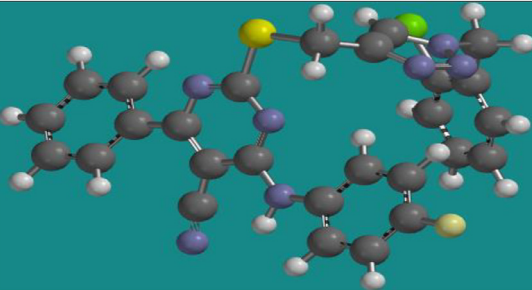| Derivatives				
Compound	R_1	R_2	R_3	Compound Name
L1	p-OCH$_3$	o-Cl	H	2-((1-(2-chlorobenzyl)-1h-1, 2, 3-triazol-4-yl)methylthio)-4-((4-methoxyphenyl)amino)-6-phenylpyrimidine-5-carbonitrile.
L2	m-CF$_3$	o-Cl	H	2-((1-(2-Chlorobenzyl) -1H-1, 2, 3-triazol-4-yl) methylthio) -4-phenyl-6-((3-(trifluoromethyl) phenyl) amino) pyrimidine-5-carbonitrile.
L3	o-Cl	o-Cl	H	2-((1-(2-Chlorobenzyl) -1H-1, 2, 3-triazol-4-yl) methylthio) -4-((2-chlorophenyl) amino) -6-phenylpyrimidine-5-carbonitrile.
L4	p-Cl	o-Cl	H	2-((1-(2-Chlorobenzyl) -1H-1, 2, 3-triazol-4-yl) methylthio) -4-((4-chlorophenyl) amino) -6-phenylpyrimidine-5-carbonitrile.
L5	m-Cl	o-Cl	H	2-((1-(2-Chlorobenzyl) -1H-1, 2, 3-triazol-4-yl) methylthio) -4-((3-chlorophenyl) amino) -6-phenylpyrimidine-5-carbonitrile.
L6	o-OCH$_3$	o-Cl	H	2-((1-(2-Chlorobenzyl) -1H-1, 2, 3-triazol-4-yl) methylthio) -4-((2-methoxyphenyl) amino) -6-phenylpyrimidine-5-carbonitrile.
L7	m- CH$_3$	o-Cl	H	2-((1-(2-Chlorobenzyl) -1H-1, 2, 3-triazol-4-yl) methylthio) -4-phenyl-6-(m-tolylamino) pyrimidine-5-carbonitrile.
L8	m-NO$_2$	o-Cl	H	2-((1-(2-Chlorobenzyl) -1H-1, 2, 3-triazol-4-yl) methylthio) -4-((3-nitrophenyl) amino) -6-phenylpyrimidine-5-carbonitrile.
L9	o-F	o-Cl	H	2-((1-(2-Chlorobenzyl) -1H-1, 2, 3-triazol-4-yl) methylthio) -4-((2-fluorophenyl) amino) -6-phenylpyrimidine-5Jcarbonitrile.
L10	p-F	o-Cl	H	2-((1-(2-Chlorobenzyl) -1H-1, 2, 3-triazol-4-yl) methylthio) -4-((4-fluorophenyl) amino) -6-phenylpyrimidine-5-carbonitrile.
L11	o- CH$_3$	o-Cl	H	2-((1-(2-Chlorobenzyl) -1H-1, 2, 3-triazol-4-yl) methylthio) -4-phenyl-6-(o-tolylamino) pyrimidine-5-carbonitrile.
L12	o-F	p- CH$_3$	H	4-((2-Fluorophenyl) amino) -2-((1-(4-methylbenzyl) -1H- 1, 2, 3-triazol-4-yl) methylthio) -6-phenylpyrimidine-5-carbonitrile.
L13	p- CH$_3$	p- CH$_3$	H	2-((1-(4-Methylbenzyl) -1H-1, 2, 3-triazol-4-yl) methylthio) -4-phenyl-6-(p-tolylamino) pyrimidine-5-carbonitrile.
L14	o-Cl	p- CH$_3$	H	4-((2-Fluorophenyl) amino) -2-((1-(4-methylbenzyl) -1H-1, 2, 3-triazol-4-yl) methylthio) -6-phenylpyrimidine-5-carbonitrile.
L15	p- CH$_3$	o-Cl	H	2-((1-(2-Chlorobenzyl) -1H-1, 2, 3-triazol-4-yl) methylthio) -4-phenyl-6-(p-tolylamino) pyrimidine-5-carbonitrile.
L16	p- CH$_3$	o-Cl	p-CH(CH$_3$)$_2$	2-((1-(2-Chlorobenzyl) -1H-1, 2, 3-triazol-4-yl) methylthio) -4-(4-isopropylphenyl) -6-(p-tolylamino) pyrimidine-5-carbonitrile.
L17	o-OCH$_3$	o-Cl	p-CH(CH$_3$)$_2$	2-((1-(2-Chlorobenzyl) -1H-1, 2, 3-triazol-4-yl) methylthio) -4-(4-isopropylphenyl) -6-(p-tolylamino) pyrimidine-5-carbonitrile.
18	p-CH$_3$	o-Cl	p-CH$_3$	2-((1-(2-Chlorobenzyl) -1H-1, 2, 3-triazol-4-yl) methylthio) -4-(p-tolyl) -6-(p-tolyamino) pyrimidine-5-carbonitrile.
L19	p- CH$_3$	o-Cl	m, p, m-triOCH$_3$	2-((1-(2-Chlorobenzyl) -1H-1, 2, 3-triazol-4-yl) methylthio) -4-(p-tolylamino) -6-(3, 4, 5-trimethoxyphenyl) pyrimidine-5-carbonitrile.
L20	p- CH$_3$	o-Cl	p-Cl	2-((1-(2-Chlorobenzyl) -1H-1, 2, 3-triazol-4-yl) methylthio) -4-(4-chlorophenyl) -6-(p-tolylamino) pyrimidine-5-carbonitrile.

Table 2
Predicted and experimental IC_{50} for EC-109 of the compound **L1- L20**.

S/N	Compounds	Predicted IC_{50}	Experimental IC_{50}
L1		7.94	7.96
L2		32.09	31.98
L3		28.29	28.45
L4		1.08	1.42
L5		24.57	24.39
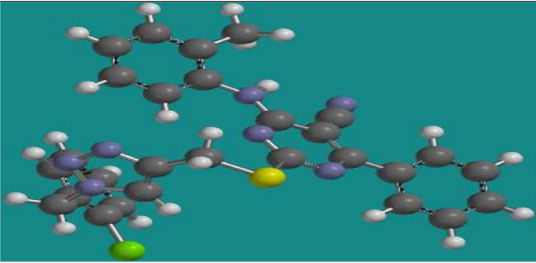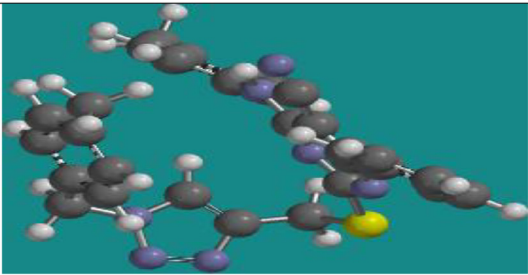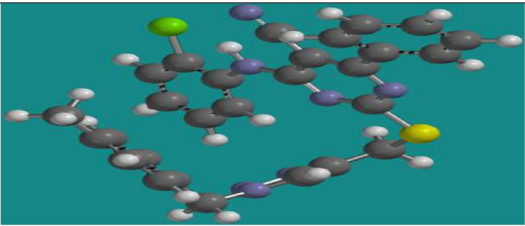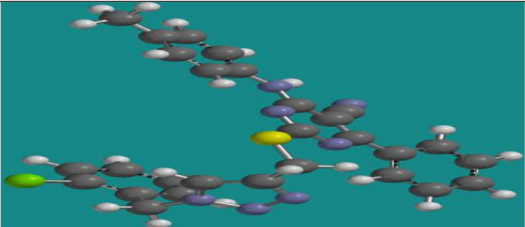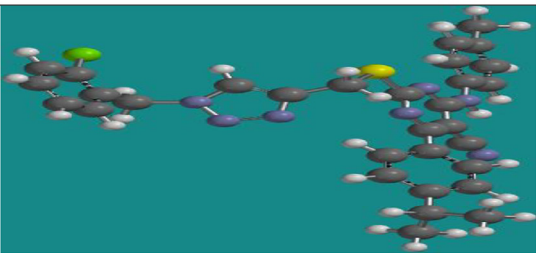
Table 2 (*continued*)

L6		9.75	9.67
L7		15.83	15.57
L8		64.02	64.00
L9		22.50	23.04
L10		25.99	25.76
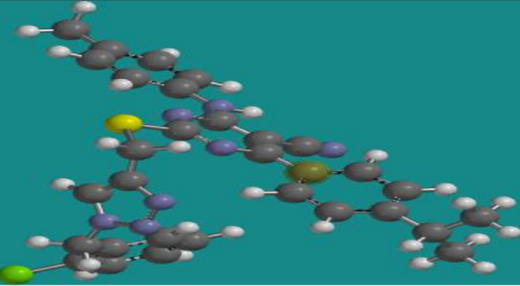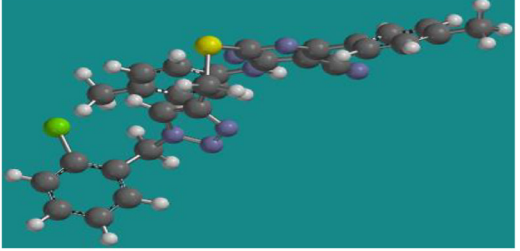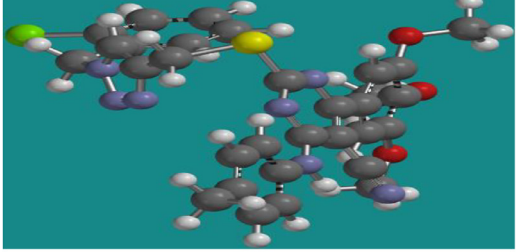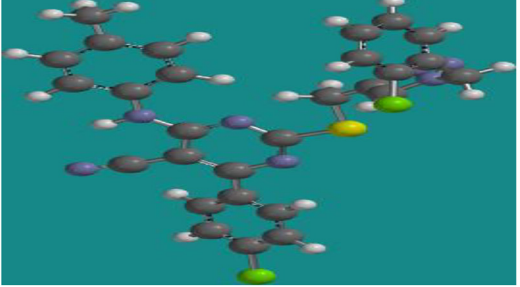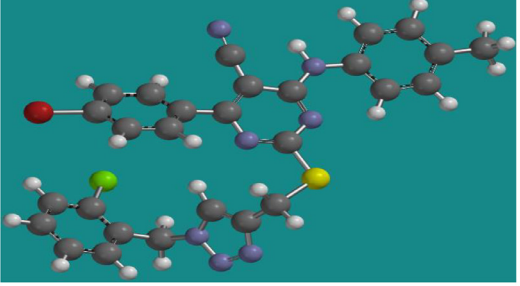
Table 2 (*continued*)

L11		9.53	9.74
L12		55.33	55.73
L13		12.11	11.22
L14		64.25	64.00
L15		5.07	5.08

Table 2 (*continued*)

L16		3.52	3.58
L17		4.62	4.65
18		5.85	5.85
L19		7.51	7.54
L20		3.12	3.09
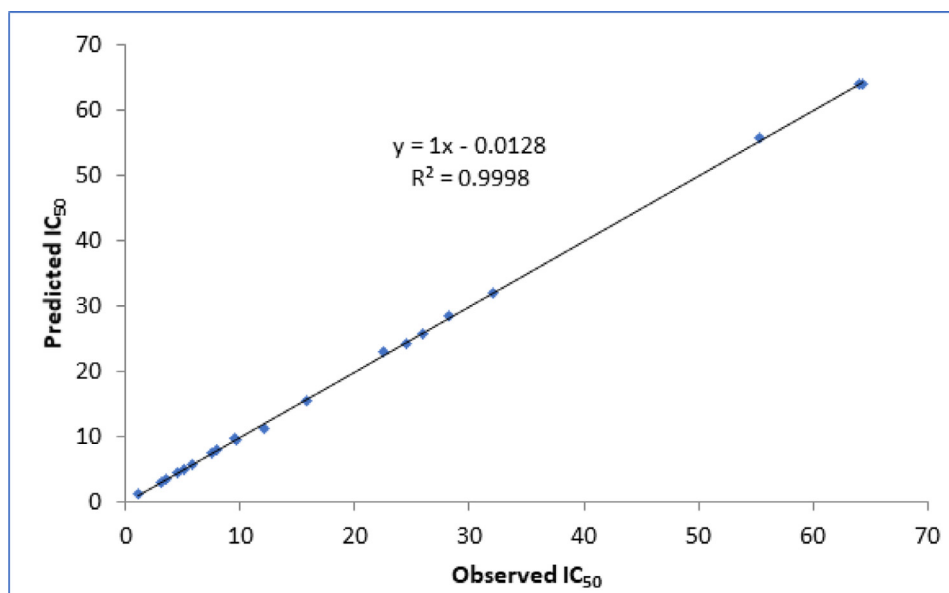
Fig. 1. The correlation between observed and predicted IC_{50} for EC-109.

Table 3
The QSAR model equation for EC-109.

Eq. (1)	N	P	R^2	CV. R^2	R_a^2
$5240.36 + 21.4466(HOMO) - 593.467(LUMO) + 0.680013(SE) + 1.34285(MW) - 3289.86(OVALITY) - 298.047(Log\ P) + 18.1521(DM) - 38.8328(PSA) + 9.33277(AREA) + 1410.97(HBD) + 107.061(HBA) - 50.0707\ (HET) + 2133.54\ (N1) - 2395.80\ (N2) + 2891.43 (N4) - 1797.75\ (N5) - 2397.38\ (N6) + 4966.48\ (N7)$	20	18	0.999	0.999	0.995

Fig. 2. Treatment of raw receptor.

Fig. 3. Transparent view of docked complexes showing ligand-receptor interactions in the binding pocket for the best selected active compounds (**L1, L4, L6, L11, L15, L16, L17, L18, L19** and **L20**) against EC-109 using Pymol.

[1,5,6]. While the other non-selected compounds have moderate to fair activity as presented in Fig. 4. Besides, Figs. 3 and 4 reflect the analysis of the docked complex which shows the ligand conformation in the active gouge of the receptor (EC-109).

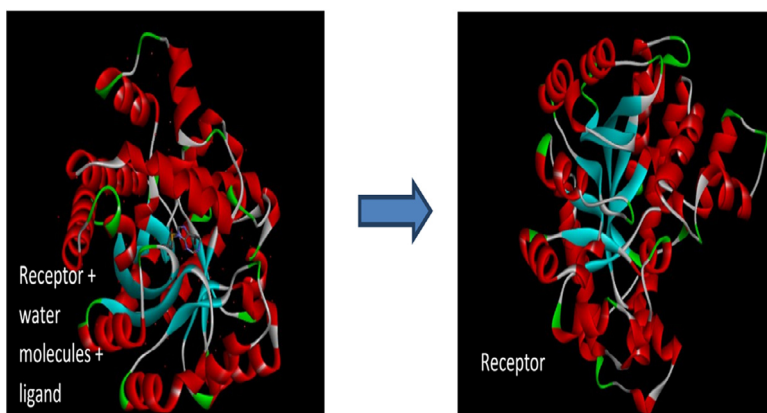Table 4 presents the datasets obtained from docking studies of the 20 compounds with their respective interactions among drug residues and EC-109; suggesting the conformation of the ligands in the active gouge of the receptor and free binding energy. Table 4 also reveals the dataset of compound **L4** as the best ligand with minimum IC_{50} and the corresponding energy interaction of free binding energy. Besides, the datasets of some compounds observed to form the number of hydrogen bonds in the gouge of the receptor are also shown in Table 4. The datasets of the compounds **L5** and **L18** that formed one hydrogen bond each are also listed in Table 4. For **L5** the hydrogen bond datasets include (SER-26, LIG: N) and (GLU-108, LIG: O) with the bond
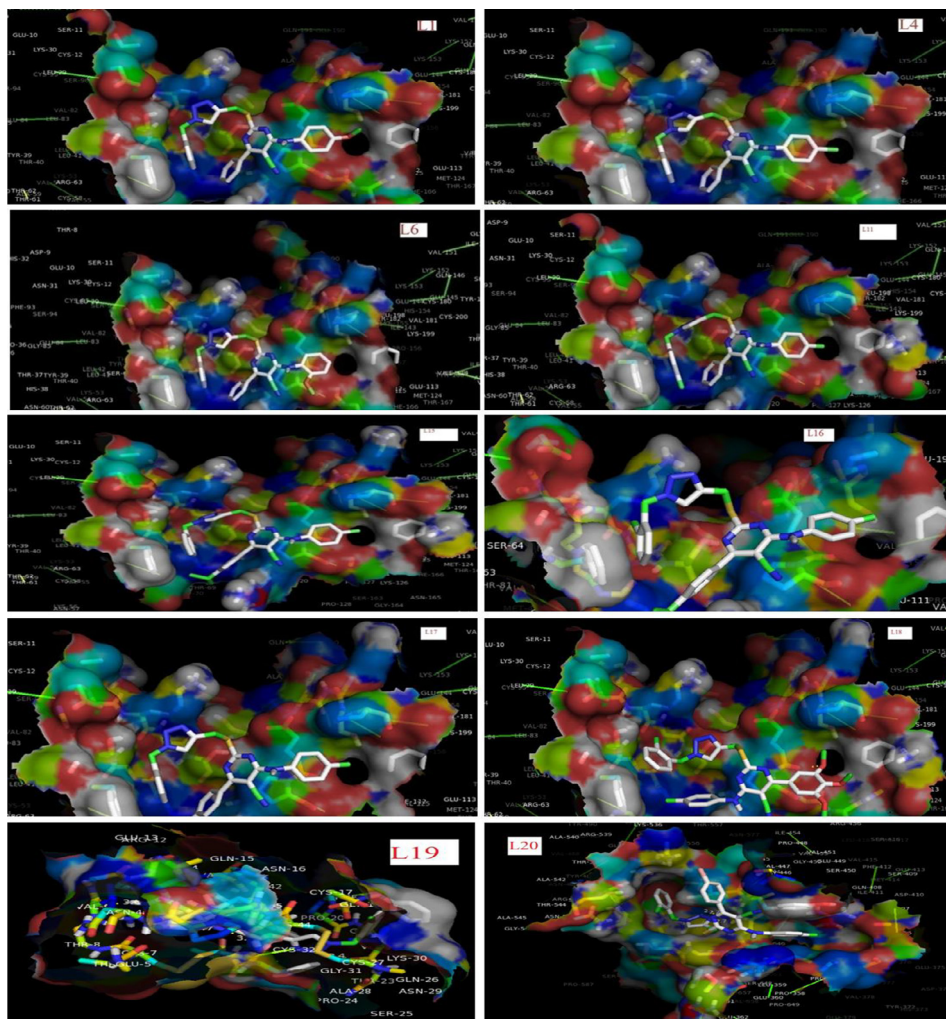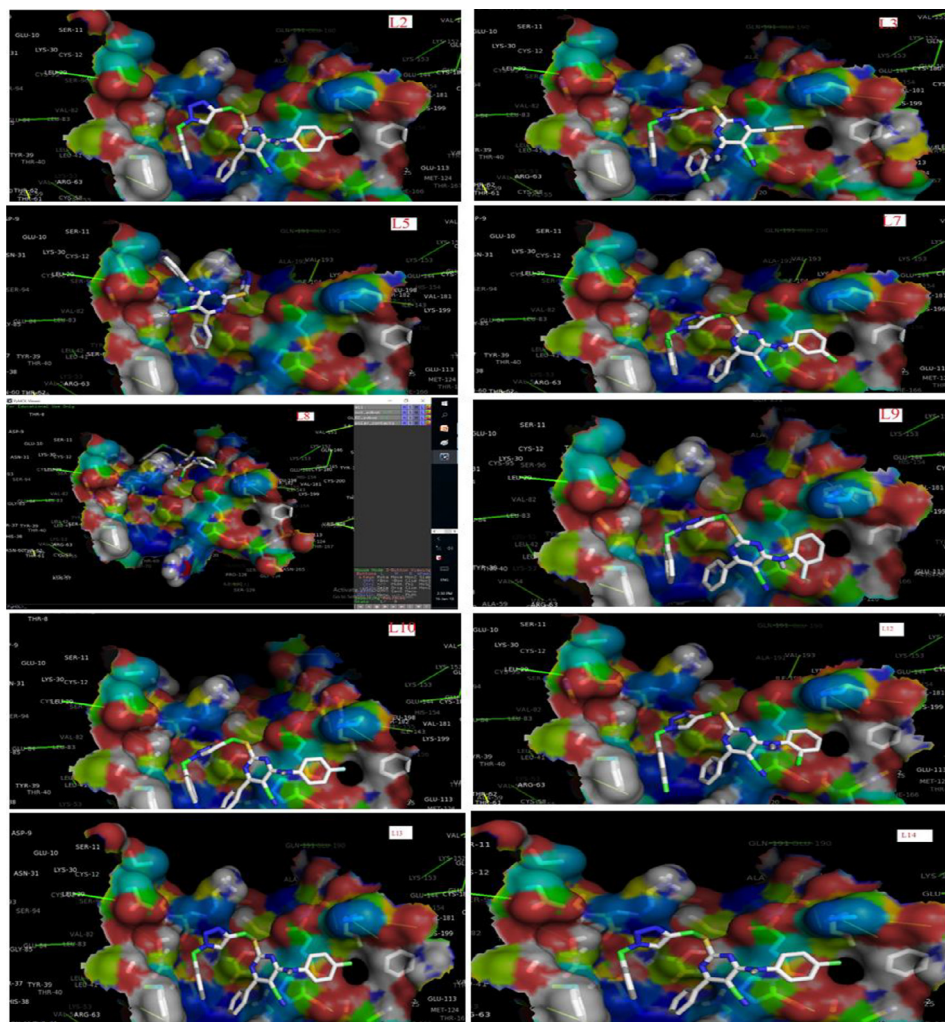
Fig. 4. Transparent view of docked complexes showing ligand-receptor interactions in the binding pocket for the non-selected compounds with moderate to fair activity against EC-109 using Pymol.

distance of 2.2 and 3.3 respectively, while L8 formed four hydrogen bonds (PHE-14, LIG: O; ILE-103, LIG: N; ASP-104, LIG: N; SER-106, LIG: H) with bond distance 2.9, 3.6, 3.4, 2.1 respectively (Table 4). The datasets of compounds **L1-L4, L6-L7, L9-L19,** and **L20** presented in Table 4 were with neither hydrogen bonding nor any bond distance. Although, there are still many other non-bonding interactions (π-π, cationic-π, anionic-π) that can occur in ligand-receptor interactions in which hydrogen bonding is just one of the interactions that predominate with EC-109.

Fig. 5 presents the correlation and relation between the IC_{50} and binding energy of the compounds **L1, L4, L6, L11, L15-L20** against EC-109 due to their higher binding free energy than **5-Fu**. They follow the sequence **L4 > L20 > L16 > L17 > L15 > L18 > L19 > L1 > L6 > L11 > 5-Fu** in the order of increased IC_{50} and decreased binding energy.

Table 4
Interactions among residues of drugs and EC-109.

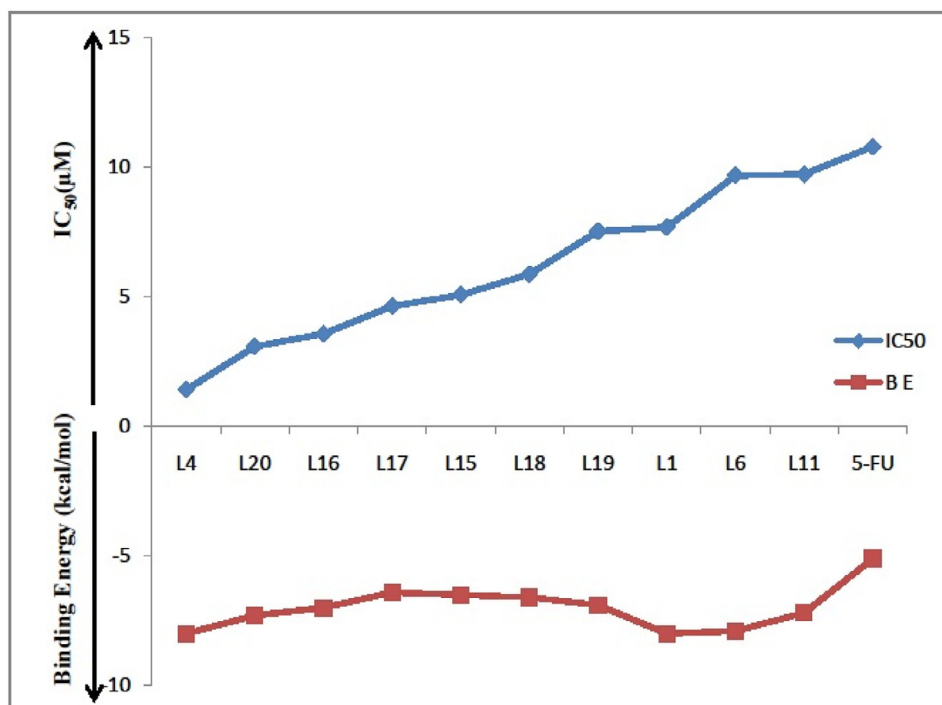| Mol	Binding Energy (kcal/mol)	IC$_{50}$ (μM)	H-bond between amino acid and drug	Distance of H-bond between amino acid and drug (Å)
L1	−8.0	7.96	–	–
L2	−8.5	31.98	–	–
L3	−8.2	28.45	–	–
L4	−8.0	1.42	–	–
L5	−6.8	24.39	SER-26, LIG: N	2.2
L6	−7.9	9.67	–	–
L7	−8.1	15.57	–	–
L8	−8.4	64	(i) PHE-14, LIG: O (ii) ILE-103, LIG:N (iii) ASP-104, LIG: N (iv) SER-106, LIG: H	2.9, 3.6, 3.4, 2.1
L9	−8.1	23.04	–	–
L10	−6.7	25.76	–	–
L11	−7.9	9.74	–	–
L12	−6.0	55.73	–	–
L13	−6.7	11.22	–	–
L14	−6.1	64	–	–
L15	−6.5	5.08	–	–
L16	−7.0	3.58	–	–
L17	−6.4	4.65	–	–
L18	−6.6	5.85	GLU-108, LIG: O	3.3
L19	−6.9	7.54	–	–
L20	−7.3	3.09	–	–
5-Fu	−5.1	10.81		

Fig. 5. Relationship between the IC$_{50}$ and binding energy of **L1, L4, L6, L11, L15, L16, L17, L18, L19** and **L20** compounds against EC-109.

2. Materials, methods and experimental design

2.1. Materials

The materials used in this work were Spartan'14 software for geometry analysis and optimization of the ligand in calculating quantum chemical process, QSAR model was obtained by Gretl software, docking study was carried out through different software such as Discovery studio 4.1 (used for the initial preparation of both receptor visualization and ligand exploration), autodock tool 1.5.6 (used to set grid box on the binding site around the compound) and autodock vina 1.1.2 (for binding energy evaluation and docking) while pymol 1.7.4.4 was used for molecular visualizations.

2.2. Minimization and optimization

The used of quantum calculations for molecular descriptor were performed using the hybrids of 1, 2, 3-triazole-pyrimidine which comprises 20 derivatives obtained from the previous work [1]. Optimization was performed on the compounds using DFT with the standard 6–31G** (d, p) basis set. Three parameters including the Becke gradient exchange correction [7], the Lee, Yang, and Parr correlation functionals (i.e. B3LYP) [8]. Molecular descriptors generated from the molecules investigated and were used to develop QSAR model in describing the bioactivity and binding affinities upon the docking of the molecules with the receptors

2.3. Molecular descriptors

The molecular descriptor is usually extracted from the electronic property of the compounds under investigation. Descriptors used in the present work includes the HOMO, LUMO, HOMO-LUMO, chemical hardness, band gaps, solvation energy, chemical potential, area volumes, diploe moments, softness, global nucleophilicity, ovality, log P, polarizability, and polar surface area. The chemical hardness, η, for an N-electron system with total energy E and η was expressed as:

$$\eta = \left(\frac{\delta^2 E}{\delta N^2} \right)_{v(r)} \approx \frac{1}{2}(IE - EA) \approx \frac{1}{2}(E_{LUMO} - E_{HOMO}) \tag{2}$$

Where IE is the vertical ionization energy approximated as -E_{HOMO} and EA for the vertical electron affinity as -E_{LUMO} [9]. The global softness is defined as the inverse of chemical hardness($S = \frac{1}{\eta}$). The electron affinity can also be used in combination with IE to give electronic chemical potential μ, negative of electron affinity (-χ) defined by Zhou et al. [10,11], as the characteristic of electronegativity of molecules:

$$\chi = -\mu = \left(\frac{\delta E}{\delta N} \right)_{v(r)} \approx \frac{1}{2}(IE + EA) \approx -\frac{1}{2}(E_{HOMO} + E_{LUMO}) \tag{3}$$

The global electrophilicity index ω introduced by Parr et al. [11], was calculated using the relation between the electronic chemical potential μ and chemical hardness η:

$$\omega = \frac{\mu^2}{2\eta} \tag{4}$$

According to the definition, the index measures the tendency of a species to accept an electron. It has been reported that high electrophilicity and nucleophilicity of a heterocycle corresponds to the extreme opposite scales of the global reactivity index [12,13]. Good electrophiles can be considered when the values of μ and ω are high, whereas, good and better reactive nucleophiles are obtained when the values of μ and ω are lower.

2.4. Validation of QSAR model

The QSAR model generated in this work was validated using statistical equations. Cross-validation (R^2) and Adjusted R^2 were considered suitable. Cross-validation governs the reliability of the QSAR model to be used for specific sets of data. In addition, it was employed as an analytical tool for estimating the prognostic/predictive controls of the equation.

$$CV.R^2 = 1 - \frac{\sum (Y\,obs - Y\,cal)^2}{\sum (Y\,obs - \bar{Y}\,obs)^2} \quad R_a^2 = \frac{(N-1) \times R^2 - P}{N-1-P} \tag{6}$$

The model is regarded as prognostic, if $R^2_{Pred} > 0.6$. However, R^2 is the coefficient of multiple determinations for multiple regressions. R^2 measures the closeness of the data to the fitting of the regression line. The better fit of R^2 value is judged by its closeness to unity (i.e. 1)

2.5. Molecular docking and binding energy evaluation

Molecular docking interaction typically brings about the formation of stable protein-protein or protein-ligand complexes which is essential for carrying out the biological functions. Therefore, it helps to predict the receptor-ligand complex conformation. It explains the relations of *y*-variable to two or more *x*-variables (or the transformation of *x*-variables). Thus, Gretl software was employed in this work to generate an equation which is given as:

$$Y = \alpha + \beta X + \varepsilon \tag{7}$$

Where *X* is the regressor (also known as the predictor or independent variable), *Y* is the response (also known as the dependent variable), the parameters; α and β describe the relations of *X* with *Y* and the term ε signifies the error model (the error is also called the residual) [14]. Thus, R^2 is considered to determine the efficiency and linearity of the analysis.

2.5.1. Discovery studio

This is software used for the simulation of the molecules and used to prepare (to remove water molecules and another residue(s) apart from the target compounds) the ligands and the receptors before subjecting them to docking studies with the autodock tool software as shown in Fig. 2.

2.5.2. Autodock

Autodock tool was designed for simulation of how small molecules including the substrates or drug candidates bind to the receptors of known 3-D structure. It further helps in locating the active binding sites (gorges) in the receptors. Based on these important features, we used Autodock Vina, a new generation of docking software from the molecular graphic laboratory. To achieve the desired goal, the required commands are as follows: vina –config conf.txt –log log.txt to do the calculations and vinasplit –input out.pdbqt to split the result in order of the scoring. Lastly, Pymol, which is a post-docking software was employed for viewing the conformation and hydrophobic interaction of the ligand and the receptor (EC-109).

Declaration of Competing Interest

There is no competing interest to declare.
This work receives no financial support from any institution or any agency.

Authors contribution

Rhoda Oyeladun Adegoke contributed to materials, performed the experiments, analyzed and interpreted the data and wrote the manuscript, Abel Kolawole Oyebamiji contributed to data analysis and interpretation and Banjo Semire conceived the experiment, contributed to materials and supervised the work.

Acknowledgments

The authors appreciate the P/A Chemistry department for the platform provided to perform the research.

Supplementary materials

Supplementary material associated with this article can be found, in the online version, at doi:10.1016/j.dib.2020.105963.

References

[1] L.Y. Ma, L.P. Pang, B. Wang, M. Zhang, B. Hu, X. Deng-Qi, S.K. Peng, B.L. Zhang, Y. Liu, E. Zhang, H.M. Liu, Design and synthesis of novel 1, 2, 3-triazole-pyrimidine hybrids as potential anticancer agents, Eur. J. Med. Chem. 86 (2014) 368–380, doi:10.1016/j.ejmech.2014.08.010.

[2] R.O. Oyewole, A.K. Oyebamiji, B. Semire, Theoretical calculations of molecular descriptors for anticancer activities of 1, 2, 3-triazole-pyrimidine derivatives against gastric cancer cell line (MGC-803): DFT, QSAR and docking approaches, Heliyon 6 (2020) e03926, doi:10.1016/j.heliyon.2020.e03926.

[3] Y. Marrero Ponce, J.A. Castillo Garit, F. Torrens, V. Romero Zaldivar, E.A. Castro, Atom, atom-type, and total linear indices of the "molecular pseudograph's atom adjacency matrix": application to QSPR/QSAR studies of organic compounds, Molecules 9 (2004) 1100–1123, doi:10.3390/91201100.

[4] A. Omotayo, A.K. Oyebamiji, O.R. Oyewole, B. Semire, A DFT-based QSAR and molecular docking studies on potent anti-colon cancer activity of pyrazole derivatives, Glob. J. Med. Res. Pharma. Drug Discov. Toxicol. Med. 18 (2018) 9–21.

[5] R.L. Walsky, A.V. Astuccio, R.S. Obach, Evaluation of 227 drugs for in vitro inhibition of cytochrome P450 2B6, J. Clin. Pharmacol. (2006), doi:10.1177/0091270006293753.

[6] H.T. Abdel-Mohsen, F.A.F. Ragab, M.M. Ramla, H.I. El Diwani, Novel benzimidazole-pyrimidine conjugates as potent antitumor agents, Eur. J. Med. Chem. (2010), doi:10.1016/j.ejmech.2010.02.011.

[7] A.D. Becke, Density-functional thermochemistry. III. The role of exact exchange, J. Chem. Phys. 98 (1993) 5648–5652, doi:10.1063/1.464913.

[8] L. Yang, J.K. Feng, A.M. Ren, Theoretical studies on the electronic and optical properties of two thiophene-fluorene based π-conjugated copolymers, Polym. Guildf 46 (2005) 10970–10981, doi:10.1016/j.polymer.2005.09.050.

[9] T. Koopmans, Über die zuordnung von wellenfunktionen und eigenwerten zu den einzelnen elektronen eines atoms, Physica 1 (1934) 104–113, doi:10.1016/S0031-8914(34)90011-2.

[10] Z. Zhou, H.V. Navangul, Absolute hardness and aromaticity: MNDO study of benzenoid hydrocarbons, J. Phys. Org. Chem. 3 (1990) 784–788, doi:10.1002/poc.610031203.

[11] R.G. Parr, L.V. Szentpály, S. Liu, Electrophilicity index, J. Am. Chem. Soc. 121 (1999) 1922–1924, doi:10.1021/ja983494x.

[12] E. Domingo, C.M. Ruiz-Jarabo, S. Sierra, A. Arias, N. Pariente, E. Baranowski, C. Escarmís, Emergence and selection of RNA virus variants: memory and extinction, Virus Res. 82 (2001) 39–44, doi:10.1016/S0168-1702(01)00385-9.

[13] E. Domingo, Quasispecies theory in virology, J. Virol. 76 (2002) 463–465, doi:10.1128/jvi.76.1.463-465.2002.

[14] R. Nicholls, Tutorial 6 : Linear Regression, (2014) 1–14.